Z. Kristallogr. Suppl. **26** (2007) 339-344

X-ray studies of nanostructured metals processed by severe plastic deformation

A.R. Kilmametov[a]*, A.V. Khristoforov[a], G. Wilde[b] and R.Z. Valiev[a]

[a]Institute of Physics of Advanced Materials, Ufa State Aviation Technical University, K. Marx st., 12, Ufa, 450000 Russia
* e-mail: ascar@mail.rb.ru or askar.kilmametov@int.fzk.de
[b]Institute of Materials Physics, University of Münster, D-48149 Münster, Germany

Keywords: severe plastic deformation, nanostructured materials, phase transformation.

Abstract. Severe plastic deformation (SPD), namely high pressure torsion (HPT), has been used to perform nanostructured states in pure Ti and Ni. Present X-ray investigations revealed that severe deformation under high imposed pressure leads not only to substructure refinement but also to accelerated $\alpha \rightarrow \omega$ phase transformation at room temperature. The ω-phase formation has been significantly affected by shear strain and applied pressure increase. The crystallite size distribution and the dislocation arrangement parameters of nanocrystalline Ni were found to be dependent on total strain level, temperature and strain rate during HPT as well as on the choice of the initial state (nanocrystalline or coarse-grained) before HPT.

Introduction

Last decade ultrafine-grained and nanocrystalline materials have been the subject of considerable research interest due to their altered physical and mechanical properties [1, 2]. Development of a number of synthesis methods [1, 3] resulted specific microstructure peculiarities of nanostructured metals in each separate case; however, the principal changes in fundamental properties are connected with extremely small grain size and increased volume fraction of grain boundaries. The use of severe deformation under high applied pressure, well-known as high pressure torsion (HPT) technique, has a potential for successive refinement in pure metals up to ~100 nm and performing of highly distorted non-equilibrium grain boundary regions [1, 4]. Recently it was revealed [5] that the combination of HPT with other methods for nanomaterials performing has an especial research potential. Initially nanocrystalline samples subjected to HPT considered being the most attractive in understanding of unusual deformation behaviour of the bulk nanostructured materials [6, 7]. On the other hand, the HPT processing parameters such as total strain level, temperature and strain rate, applied pressure strongly influence microstructure characteristics. Specific distribution of crystallographic defects can be accompanied also by alterations of phase composition, increased solubility of alloying elements, etc. [1, 2]. As is well known, Ti subjected to high pressure

has a more open hexagonal structure (ω phase, A1B2 type), which is metastable after pressure removal in ambient conditions [8]. However, the lack of experimental data dealing with HPT-induced phase transition and orientation relationships between noted phases initiated the X-ray studies resulted in the present paper. Therewith, microstructure parameters of nanocrystalline Ni, namely, the values of grain size, their distribution and the dislocation structure in terms of density, arrangement parameter and preferable character of dislocation have been investigated in dependence on HPT processing conditions.

Experimental

HPT was used to process nanostructured states in commercially pure coarse-grained Ti and nanocrystalline Ni. The disk-shape samples of commercial purity Ti have been processed by means of HPT deformation under the quasi-hydrostatic pressure P equal to 3, 4, 5 and 6 GPa for 5 rotations (N = 5) and P = 6 GPa for 0.5, 1, 5 and 10 rotations (N = 0.5-10) at a strain rate of 1 rotation per minute (rpm). Nanocrystalline Ni was prepared by repeated cold- rolling and folding (F&R) procedure [9] and subsequently subjected to HPT at 20°C with 1 rpm; at 100°C with 1 and 0.1 rpm. The X-ray structural investigations were performed in Bragg-Brentano focusing geometry using the Cu K_α radiation and graphite monochromator <0002> for the diffracted beam. Measurement data were recorded in the scanning step equal to 0.02° and the counting time equal to 20 seconds at each point. The modified Williamson-Hall and the modified Warren-Averbach procedures [10] were used to obtain microstructure characteristics of nanocrystalline Ni.

Results and discussion

HPT titanium. The X-ray diffraction patterns of the initial coarse-grained sample and HPT-deformed ones at 3 and 6 GPa are presented in figure 1. One can see a number of diffraction peaks typical for α- Ti with h.c.p. crystalline lattice (figures 1a, b). The peak profiles of the HPT Ti are considerably broadened and intensity of some peaks becomes comparable with diffuse scattering background. The redistribution of integral peak intensity followed by HPT at P=3 GPa (figure 1, b) testifies to shear texture formation with strong <0001> component. The increase in applied pressure during HPT up to 4÷6 GPa (figure 1, c) resulted in partial transition of the α-phase into the high-pressure ω-phase. As it can be seen in figure 2 a volume fraction of the ω-phase depends both on applied pressure with the given accumulated shear strain and on shear strain with the given pressure value. A strong deformation texture preceding the α→ω transformation led to increased amount of basal atomic layers of α-phase situated in the shear plain. Figure 3 demonstrates the dependence of the integral intensity peak's relation I $(0002)_\alpha$ / I $(10\bar{1}1)_\alpha$ on volume fraction of ω-phase which has been appeared. One can see that the I $(0002)_\alpha$ / I $(10\bar{1}1)_\alpha$ value which characterizes texture state of α-phase during transformation remains nearly the same whereas the amount of ω-phase is increasing from zero till 65÷70 %. This fact is in a good agreement with theoretical prediction that α→ω transformation results from atomic shuffles in $(0001)_\alpha$ planes [11]. The formation of the basal texture in α-phase prior its transformation to ω-phase allows us to expect that the new ω-grains also have preferable orientations according to existing orientation

relationships between these two phases. Though a rather symmetrical $(10\bar{1}0/11\bar{2}0)_\omega$ peak is not properly distinguished into two diffraction peaks, intensity of the $(22\bar{4}0)_\omega$ peak appears to be significantly increased in comparison with the others (Table 1).

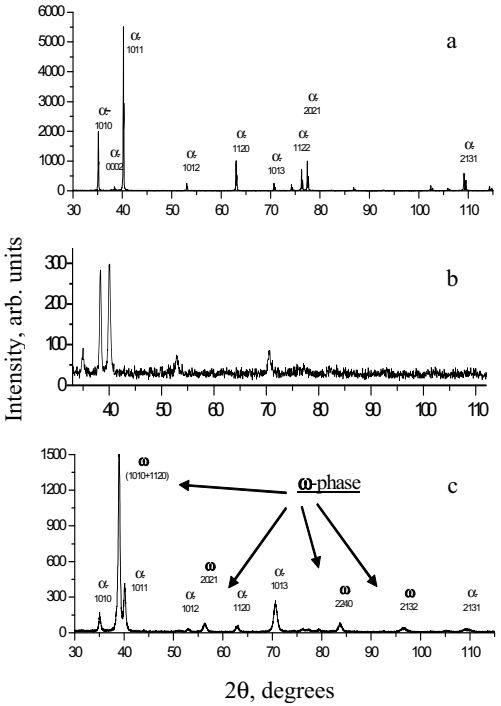

Figure 1. The X-ray diffractogram of Titanium: initial state(a); after HPT deformation under applied pressure of P = 3 GPa (b) and P = 6 GPa (c)

As far $(11\bar{2}0)_\omega$ and $(22\bar{4}0)_\omega$ peaks are attributed to different diffraction orders of the same crystallographic planes, the $(11\bar{2}0)_\omega$ atomic layers are assumed to be preferable in the ω-phase after transformation. Therefore the $(0001)_\alpha \parallel (11\bar{2}0)_\omega$ orientation relation for atomic planes could be concluded as the most probable in the case of shear strain induced phase transformation after HPT. The possibility of this phase relationship was discussed previously [11] but, to our best knowledge, has not been established as the HPT-induced consequence yet. The results obtained clearly indicate the formation of ω-phase in titanium at HPT deformation already under a pressure of 4 GPa. Obviously, the reason for accelerated formation of the ω-phase is related to a considerable change of the driving force provided by the external shear stress.

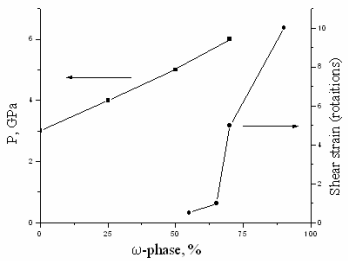

Figure 2. An ω-phase volume fraction dependences on applied pressure (n=const) and shear strain (P=const) during HPT

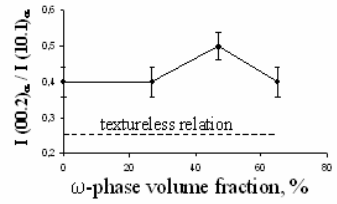

Figure 3. Integral intensity relations of the α-phase peaks in dependence on the ω-phase volume fraction

Table 1. The ω-phase parameters resulted by HPT-induced transformation at P=6 GPa.

HKWL	2 Θ, degrees	Relative intensity (experimental), %	Relative intensity (textureless), %
$10\bar{1}0$	38.97	≈100	89
$11\bar{2}0$	39.01	≈100	100
$20\bar{2}1$	56.35	19.6	27.5
$22\bar{4}0$	83.75	15.9	8.5
$21\bar{3}2$	96.61	13.2	11.5

HPT nickel. X-ray peak profile analysis by means of *modified* Williamson-Hall and *modified* Warren-Averbach procedures allowed revealing microstructure peculiarities of nanocrystalline Ni states processed at different HPT regimes (Table 2). A log-normal size distribution was calculated for investigated states (figure 4). Crystallite size values (d, L_0), dislocation arrangement characteristics (q, ρ and M) and crystallite size distribution parameters (m and σ) has been affected by total accumulated strain after severe deformation as well as temperature and strain rate during HPT. One can see that subsequent (F&R+HPT) processing resulted both in crystallite size decrease and the dislocation density increase. The last ones surge to extremely high values in contradiction to insignificant size changes. Elevated temperature and smaller strain rate of HPT lead to dislocation density decrease. Similar value $\rho \approx 2 \times 10^{16}$ (m^{-2}) has been reported in the case of ball milled Ni [12]. Thereby the level of

dislocation density equal to (2÷5) $\times 10^{16}$ (m^{-2}) assumes to be the highest, which might be achieved in bulk Ni samples by SPD. The experimental q parameters [16] obtained for (F&R+HPT) states reveals preferable screw dislocation character (Table 2). Decrease of the noted values from maxima corresponding to HPT at room temperature shows that composed screw and edge type takes place in the case of elevated temperatures and/or reduced strain rate of HPT processing. Note the HPT refinement from the coarse-grain structure results in preferable edge dislocation type. As was published earlier [13, 14], screw dislocations annihilate more effectively than edge ones in f.c.c. metals with increase of deformation stage at low temperatures. In our case of the initially nanocrystalline F&R samples the (F&R+HPT) application leads to much higher total accumulated strain in comparison with "traditional" HPT refinement. Dynamic interaction between lattice dislocations and non-equilibrium grain boundaries during SPD performs enough complicate defect structure in the material, where highly distorted areas appear to be the sources of the long-range internal fields. In this connection, analysis of the dislocation arrangement parameter M implements the X-ray data concerning dislocation structure of the HPT Ni. Parameter M (Table 2)

Table 2. Microstructure parameters of nanocrystalline Ni.

	d, (nm)	L_0, (nm)	q	ρ, $\times 10^{15}$ (m^{-2})	M	m, (nm)	σ
F&R	23.3	22.2	2.08	6.4	3.9	17.9	0.23
F&R+HPT, 20°C, 1rpm	17.3	14.5	2.23	53.8	2.3	9.3	0.42
F&R +HPT, 100°C, 1 rpm	18.5	17.7	1.98	20.0	2.8	16	0.17
F&R +HPT, 100°C, 0.1 rpm	20.7	19.4	1.7	16.6	3.3	17	0.25
HPT (conventional), 20°C, 1rpm	55.5	47.4	1.6	4.8	0.3	31.7	0.4

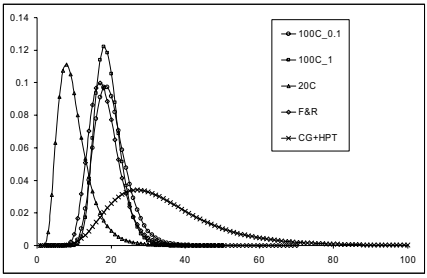

Figure 4. The crystallite size distribution in HPT Ni.

increases if the long-range character of the strain field of dislocation increases. Strong or week screening of the displacement field of dislocations results in small or large values of M, respectively [14]. High total strain accumulated after both F&R and (F&R+HPT) treatments results in elevated parameter M. Severe shear deformation from coarse-grain state gives the parameter M less in order of magnitude than others (Table 2) and testifies significant screen-

ing effect. This fact correlates with similar *M* values equal to fractions of unit [13] which were attributed to subgrain structure divided by a dislocation network.

Conclusions

The unique combination of microstructure features of SPD materials (very small grain size, high elastic lattice stresses and non-equilibrium grain boundaries) assumes to be a key factor to exceed phase transition in titanium by shear deformation. Probably, a high level of free energy as well as heterogeneous distribution of crystalline defects in different texture components results in the polymorphous transformation in HPT Ti.

The present results obtained by modified X-ray diffraction procedures shows that HPT-induced microstructure characteristics of bulk nanocrystalline Ni are in significant dependence on temperature and strain rate conditions of HPT processing as well as the choice of initial (nanostructured by F&R treatment or coarse-grained) state before HPT. Total strain accumulated by (F&R+HPT) application results in extremely high level of internal stress fields considered to be the ultimate in severely deformed bulk samples.

References

1. Valiev, R.Z., Islamgaliev, R.K., Alexandrov I.V., 2000, *Progr. in Mat. Sci.*, **45,** 103.
2. Valiev, R.Z., 2004, *Nature Materials*, **3**, 511.
3. Suryanarayana, C., 2001, *Progr. in Mater. Sci.*, **46**, 1.
4. Zhu, Y. T. & Butt, D. P., 2004, in *Encyclopedia of Nanotechnology*, **6**, edited by H. S. Nalwa (American Scientific, Stevenson Ranch, CA), 843.
5. Wilde, G., Boucharat, N., Hebert, R., Rösner, H., Valiev, R., 2006, *Mat. Sci. Eng. A*, (in press)
6. Markmann, J., Bunzel, P., Rősner, H., Liu, K.W., Padmanabhan, K.A., Birringer, R., Gleiter, H., Weissműller, J., 2003, *Scripta Mat*., **49**, 637.
7. Liao, X. Z., Kilmametov, A.R., Valiev, R. Z., Gao, H. S., Li, X. D., Mukherjee, A. K., Bingert, J. F., Zhu, Y. T., 2006, *Appl. Phys. Lett.*, **88**, 021909.
8. Errandonea, D., Meng, Y., Somayazulu, M., Häusermann, D., 2005, Physica B, **355**, 116.
9. Dinda, G.P., Rösner, H., Wilde, G., 2005, *Mater, Sci. Eng.* **A** 410-411, 328.
10. Ungár, T. & Borbély, A., 1996, *Appl. Phys. Lett.*, **69**, 3173.
11. Silcock, J. M., 1958, *Acta Metall.*, **6**, 481.
12. Scardi, P.& Leoni, M., 2002, *Acta. Cryst. A*, **58,** 190.
13. Zehetbauer, M., Ungar, T., Kral, R., Borbely, A., Schafler, E., Ortner, B., Amenitsch, H., Bernstorff, S., 1999, *Acta Mater.*, **47**, 3, 1053.
14. Ungár, T., Gubicza, J., Ribarik, G. & Borbély, A., 2001, *J. Appl. Cryst.*, **34**, 298.

Acknowledgements. This work was partially supported by the US DOE IPP program under the project LANL-T2-199.